FTIR-ATR Study of Water Uptake and Diffusion through Ion-Selective Membranes Based on Poly(acrylates) and Silicone Rubber

ARTICLE *in* ANALYTICAL CHEMISTRY · JULY 2009

Impact Factor: 5.64 · DOI: 10.1021/ac900727w · Source: PubMed

Anal. Chem. **2009,** *81,* 5925–5934

FTIR-ATR Study of Water Uptake and Diffusion through Ion-Selective Membranes Based on Poly(acrylates) and Silicone Rubber

Fredrik Sundfors,[†] Tom Lindfors,*[,†] Lajos Höfler,[‡] Róbert Bereczki,[‡] and Róbert E. Gyurcsányi*[,‡,§]

Process Chemistry Centre, Laboratory of Analytical Chemistry, Åbo Akademi University, Biskopsgatan 8, FI-20500 Åbo/Turku, Finland, Department of Inorganic and Analytical Chemistry, Budapest University of Technology and Economics, H-1111 Budapest, Szt. Gellért tér 4, Hungary, and Research Group of Technical Analytical Chemistry, Hungarian Academy of Sciences, Budapest University of Technology and Economics, H-1111 Budapest, Szt. Gellért tér 4, Hungary

For the first time, FTIR-ATR spectroscopy was used to study the water uptake and its diffusion in ion-selective membranes (ISMs) based on poly(acrylates) (PAs) and silicone rubber (SR), which are emerging materials for the fabrication of ISMs for ultratrace analysis. Three different types of PA membranes were studied, consisting of copolymers of methyl methacrylate with *n*-butyl acrylate, decyl methacrylate, or isodecyl acrylate. Numerical simulations with the finite difference method showed that in most cases the water uptake of the PA and SR membranes could be described with a model consisting of two diffusion coefficients. The diffusion coefficients of the PA membranes were approximately 1 order of magnitude lower than those of plasticized poly(vinyl chloride) (PVC)-based ISMs and only slightly influenced by the membrane matrix composition. However, the simulations indicated that during longer contact times, the water uptake of PA membranes was considerably higher than that for plasticized PVC membranes. Although the diffusion coefficients of the SR and plasticized PVC membranes were similar, the SR membranes had the lowest water uptake of all membranes. This can be beneficial in preventing the formation of detrimental water layers in all-solid-state ion-selective electrodes. With FTIR-ATR, one can monitor the accumulation of different forms of water, i.e., monomeric, dimeric, clustered, and bulk water.

Plasticized poly(vinyl chloride) (PVC)[1] has traditionally been the most commonly used membrane material for potentiometric ion-selective electrodes (ISEs) and optodes.[2] PVC membranes possess a rather high tensile strength, chemical inertness, and an easy preparation procedure combined with good compatibility with ionophores covering a wide variety of chemical structures. Some drawbacks of plasticized PVC membranes have been noticed very early, i.e., slow leaching of the plasticizer,[3] ionophore,[4] and other lipophilic additives from the ion-selective membrane (ISM) phase leading to decreased lifetime of the ISEs.[5] Miniaturized ISEs and optodes are clearly the most affected configurations because of the high area/volume ratio of their membranes. Beside the fact that plasticizer leaching from plasticized PVC membranes can cause inflammatory[6,7] and/or thrombogenic responses[8] during measurements in biological environments, its exudation results in reduced adhesion of the membranes when utilized within planar electrodes.[7] Later, with the use of ISEs for ultratrace analysis,[9−12] it became clear that low diffusivity membranes,[9] i.e., characterized by several orders of magnitude lower free ionophore diffusion coefficients than those of the conventional PVC-based membranes (10^{-8} cm^2s^{-1}),[13,14] lead to superior robustness of the potential response. However, not even PVC membranes with much reduced plasticizer content could meet this expectation without considerable deterioration of their selectivity.

Most recently solid contact ISEs (SC-ISEs) were recognized as probably the ultimate choice for trace analysis measurements.[15,16]

* To whom correspondence should be addressed. (T.L.) E-mail: Tom.Lindfors@abo.fi. Fax: +358-2-2154479. (R.G.) E-mail: robertgy@mail.bme.hu.
† Åbo Akademi University.
‡ Department of Inorganic and Analytical Chemistry, Budapest University of Technology and Economics.
§ Hungarian Academy of Sciences, Budapest University of Technology and Economics.

(1) Shatkay, A. *Anal. Chem.* **1967**, *39*, 1056–1065.
(2) Bakker, E.; Bühlmann, P.; Pretsch, E. *Chem. Rev.* **1997**, *97*, 3083–3132.
(3) Reinhoudt, D. N.; Engbersen, J. F. J.; Brzozka, Z.; Vandenvlekkert, H. H.; Honig, G. W. N.; Holterman, H. A. J.; Verkerk, U. H. *Anal. Chem.* **1994**, *66*, 3618–3623.
(4) Dinten, O.; Spichiger, U. E.; Chaniotakis, N.; Gehrig, P.; Rusterholz, B.; Morf, W. E.; Simon, W. *Anal. Chem.* **1991**, *63*, 596–603.
(5) Oesch, U.; Simon, W. *Anal. Chem.* **1980**, *52*, 692–700.
(6) Lindner, E.; Cosofret, V. V.; Buck, R. P.; Johnson, T. A.; Ash, R. B.; Neuman, M. R.; Kao, W. J.; Anderson, J. M. *Electroanalysis* **1995**, *7*, 864–870.
(7) Lindner, E.; Cosofret, V. V.; Ufer, S.; Buck, R. P.; Kao, W. J.; Neuman, M. R.; Anderson, J. M. *J. Biomed. Mater. Res.* **1994**, *28*, 591–601.
(8) Espadas-Torre, C.; Meyerhoff, M. E. *Anal. Chem.* **1995**, *67*, 3108–3114.
(9) Vigassy, T.; Gyurcsányi, R. E.; Pretsch, E. *Electroanalysis* **2003**, *15*, 375–382.
(10) Szigeti, Z.; Vigassy, T.; Bakker, E.; Pretsch, E. *Electroanalysis* **2006**, *18*, 1254–1265.
(11) Sokalski, T.; Ceresa, A.; Zwickl, T.; Pretsch, E. *J. Am. Chem. Soc.* **1997**, *119*, 11347–11348.
(12) Lindner, E.; Gyurcsányi, R. E.; Buck, R. P. *Electroanalysis* **1999**, *11*, 695–702.
(13) Bodor, S.; Zook, J. M.; Lindner, E.; Tóth, K.; Gyurcsányi, E. R. *J. Solid State Electrochem.* **2009**, *13*, 171–179.
(14) Bodor, S.; Zook, J. M.; Lindner, E.; Tóth, K.; Gyurcsányi, R. E. *Analyst* **2008**, *133*, 635–642.
(15) Sutter, J.; Radu, A.; Peper, S.; Bakker, E.; Pretsch, E. *Anal. Chim. Acta* **2004**, *523*, 53–59.
(16) Sutter, J.; Lindner, E.; Gyurcsányi, R. E.; Pretsch, E. *Anal. Bioanal. Chem.* **2004**, *380*, 7–14.

10.1021/ac900727w CCC: $40.75
Published on Web 06/15/2009

With these electrodes, the high water uptake of PVC[17−20] constitutes a major drawback because water accumulation on the inner side of the membrane at the SC interface can lead to drifting potential responses[21] and ultimately to the loss of the benefits of the SC configuration.[22] Most of the conventional membranes and SC materials were shown to fail the so-called aqueous layer test,[23] which is a method to detect water accumulation at the inner SC−ISM interface. In addition, although never explicitly proven, the water sorption in the membrane might have detrimental effects on the lower detection limit by increasing the extent of salt coextraction and ion mobility in the membrane. While throughout the development of ionophore-based ISEs there has been considerable interest in exploring alternative materials to plasticized PVC,[3,24,25] the search for new materials replacing PVC membranes becomes important for the fabrication of SC-ISEs suitable for ultratrace measurements. These alternative materials should provide a hydrophobic membrane matrix having a glass transition temperature well below room temperature.[26,27] Furthermore, they should show good compatibility with most of the ionophores (preserving their selectivities), low mobility of the membrane components, and preferably low water uptake.

The most established alternative ISM materials for ultratrace applications are different types of poly(acrylates) (PAs). While early attempts of using plasticized PA membranes for ISEs[28−30] did not show any improvements with respect to PVC membranes, the introduction of self-plasticized PA copolymer-based ISMs by Hall[31,32] and their refinement for low detection limit ISEs by the Bakker group[15] made PAs one of the most prospective ISM materials. These membranes are usually copolymers built of the following monomers: methyl methacrylate (MMA), *n*-butyl acrylate (NBA) and glycidyl methacrylate (GMA),[32] MMA, NBA and *n*-heptyl acrylate (NHA),[31] MMA and NBA,[32] MMA and isodecyl acrylate (IDA),[33] and MMA and decyl methacrylate (DMA).[34] The mechanical properties of PAs can be further adjusted by adding cross linkers to obtain cross-linked poly(*n*-butyl acrylate) (PNBA)[35] and poly(isodecyl acrylate) (PIDA).[36] In many cases, the PA-based ISEs were shown to have comparable[34] response characteristics compared to PVC membranes for a large number of ionophores, including those selective to Na^+,[33,37] K^+,[35,38] Li^+,[34] Ag^+,[39] Ca^{2+},[15,39] Mg^{2+},[34] Pb^{2+},[15,39] Cl^-,[40] and I^-.[39] The main advantages of the membranes listed above are that they are self-plasticizing, i.e., do not require plasticizers. In such a PA membrane (MMA:NBA), the apparent diffusion coefficients of K^+ and Na^+ were of the order of 10^{-11} to 10^{-12} cm^2 s^{-1},[41] which is approximately 3 orders of magnitude lower than those of plasticized PVC membranes. As decreasing the magnitude of zero-current ion fluxes in the membrane is beneficial for obtaining ISMs with low detection limits[9,41] significant improvements of the detection limit could be indeed robustly achieved by using ISEs based on PA membranes.[10,15,39] The rather poor mechanical strength and stickiness of many of the PA membranes restrict their use to SC-supported membrane-based electrodes. Although at present the relative contribution of the SC and of the polymeric membrane in avoiding the formation of an aqueous layer beneath the ISM is unclear, the characterization of ISMs in terms of water uptake is expected to contribute to the understanding and better design of the inner membrane interface. Therefore, because the formation of an aqueous layer is believed to originate from the water sorption of ISMs, here we report on a systematic study of the water uptake of PA and silicone rubber membranes emerging as materials for the fabrication of ISEs for ultratrace analysis.

Although the water uptake of some PAs with wide applications in dentistry and biomedical engineering[42,43] were already studied[44,45] because of the influence of absorbed water on their mechanical properties, there is a large difference in the composition of those materials and the PA membrane compositions used for ISEs. In addition, as we have shown earlier for plasticized PVC membranes, the additives used in ISEs are also expected to influence the water uptake and equilibrium water content of the PA membranes.[19] The aqueous layer test,[23] based on monitoring potential drifts as a result of transmembrane ion transport, is not really applicable for PAs because of their very low ion diffusivities, which would increase the time frame to weeks compared to hours when applied to plasticized PVC membranes. The recently proposed alternative of the potentiometric aqueous layer test, based on monitoring potential drifts as a result of the CO_2 permeation, is only applicable to pH sensitive membranes.[46]

Silicone rubber (SR)-based ISMs[47−49] show great promise for the fabrication of ISEs with ultratrace analysis capability because of their well-known water repellant and insulating properties,

(17) Armstrong, R. D.; Johnson, B. W. *Corros. Sci.* **1991**, *32*, 303–312.
(18) Li, Z.; Li, X. Z.; Petrovic, S.; Harrison, D. J. *Anal. Chem.* **1996**, *68*, 1717–1725.
(19) Lindfors, T.; Sundfors, F.; Höfler, L.; Gyurcsányi, E. R. *Electroanalysis* **2009**, accepted for publication.
(20) Thoma, A. P.; Viviani-Nauer, A.; Arvanitis, S.; Morf, W. E.; Simon, W. *Anal. Chem.* **1977**, *49*, 1567–1572.
(21) Fibbioli, M.; Morf, W. E.; Badertscher, M.; de Rooij, N. F.; Pretsch, E. *Electroanalysis* **2000**, *12*, 1286–1292.
(22) Lindner, E.; Gyurcsányi, R. E. *J Solid State Electrochem.* **2009**, *13*, 51–68.
(23) Fibbioli, M.; Bandyopadhyay, K.; Liu, S. G.; Echegoyen, L.; Enger, O.; Diederich, F.; Gingery, D.; Buhlmann, P.; Persson, H.; Suter, U. W.; Pretsch, E. *Chem. Mater.* **2002**, *14*, 1721–1729.
(24) Högg, G.; Lutze, O.; Cammann, K. *Anal. Chim. Acta* **1996**, *335*, 103–109.
(25) Kimura, K.; Sunagawa, T.; Yokoyama, M. *Anal. Chem.* **1997**, *69*, 2379–2383.
(26) Armstrong, R. D.; Horvai, G. *Electrochim. Acta* **1990**, *35*, 1–7.
(27) Heng, L. Y.; Hall, E. A. H. *Anal. Chim. Acta* **2000**, *403*, 77–89.
(28) Hassan, S.; Moody, G. J.; Thomas, J. D. R. *Analyst* **1980**, *105*, 147–153.
(29) Fiedler, U.; Ruzicka, J. *Anal. Chim. Acta* **1973**, *67*, 179–193.
(30) Mascini, M.; Pallozzi, F. *Anal. Chim. Acta* **1974**, *73*, 375–382.
(31) Heng, L. Y.; Hall, E. A. H. *Anal. Chem.* **2000**, *72*, 42–51.
(32) Heng, L. Y.; Hall, E. A. H. *Anal. Chim. Acta* **1996**, *324*, 47–56.
(33) Malinowska, E.; Gawart, L.; Parzuchowski, P.; Rokicki, G.; Brzozka, Z. *Anal. Chim. Acta* **2000**, *421*, 93–101.
(34) Qin, Y.; Peper, S.; Bakker, E. *Electroanalysis* **2002**, *14*, 1375–1381.
(35) Heng, L. Y.; Hall, E. A. H. *Anal. Chim. Acta* **2001**, *443*, 25–40.
(36) Wydgladacz, K.; Durnas, M.; Parzuchowski, P.; Brzozka, Z.; Malinowska, E. *Sens. Actuators, B* **2003**, *95*, 366–372.
(37) Grygolowicz-Pawlak, E.; Wygladacz, K.; Sek, S.; Bilewicz, R.; Brzozka, Z.; Malinowska, E. *Sens. Actuators, B* **2005**, *111*, 310–316.
(38) Heng, L. Y.; Hall, E. A. H. *Electroanalysis* **2000**, *12*, 187–193.
(39) Chumbimuni-Torres, K. Y.; Rubinova, N.; Radu, A.; Kubota, L. T.; Bakker, E. *Anal. Chem.* **2006**, *78*, 1318–1322.
(40) Lyczewska, M.; Wojciechowski, M.; Bulska, E.; Hall, E. A. H.; Maksymiuk, K.; Michalska, A. *Electroanalysis* **2007**, *19*, 393–397.
(41) Heng, L. Y.; Tóth, K.; Hall, E. A. H. *Talanta* **2004**, *63*, 73–87.
(42) Goodelle, J. P.; Pearson, R. A.; Santore, M. M. *J. Appl. Polym. Sci.* **2002**, *86*, 2463–2471.
(43) Pearson, G. J.; Braden, M. *J. Dental Res.* **1981**, *60*, 1112–1112.
(44) Iwamoto, R.; Matsuda, T. *Anal. Chem.* **2007**, *79*, 3455–3461.
(45) Sutandar, P.; Ahn, D. J.; Franses, E. I. *Macromolecules* **1994**, *27*, 7316–7328.
(46) Grygolowicz-Pawlak, E.; Plachecka, K.; Brzozka, Z.; Malinowska, E. *Sens. Actuators, B* **2007**, *123*, 480.

excellent mechanical characteristics, and good adhesion to a wide variety of substrates. Silicone rubber as an ISM matrix was introduced in 1973[49] for K^+-selective ISEs and applied later for a variety of ionophore-based sensors[47,48,50−53] but has been studied less extensively than plasticized PVC and PA membranes.

There are a number of methods for studying water uptake of polymeric materials, including simple gravimetric methods,[54] quartz crystal microbalance,[55] NMR,[56] optical waveguide spectroscopy,[57] electrochemical impedance spectroscopy,[58] and various vibrational spectroscopic methods.[59] Here, we report on the use of FTIR-ATR spectroscopy[19,60] because this technique can distinguish between different types of water: monomeric (non-hydrogen bonded or "free water"), dimeric (weakly hydrogen bonded), clustered (moderately strong hydrogen bonded), and bulk water (strongly hydrogen bonded).[45,61] This is useful for understanding the water uptake mechanism of different types of polymers. While the water uptake of nonplasticized poly(methyl methacrylate) (PMMA) has previously been studied with FTIR-ATR spectroscopy,[45] to the best of our knowledge there are no FTIR-ATR studies on the water uptake of ISMs based on different types of PAs and SRs. The present study will therefore focus on these ISM matrices in order to identify ISMs with low water uptake.

EXPERIMENTAL SECTION

Chemicals. Room temperature vulcanizing silicone rubber (RTV 3140) was obtained from Dow Corning. Bis(2-ethylhexyl) sebacate (DOS), potassium tetrakis[3,5-bis(trifluoromethyl)phenyl]borate (KTFPB), calcium ionophore I (ETH 1001), calcium ionophore IV (ETH 5234), and tetrahydrofuran (THF) were of Selectophore grade and obtained from Fluka. Methyl methacrylate (MMA), *n*-butyl acrylate (NBA), isodecyl acrylate (IDA), azobisisobutyronitrile (AIBN), and methanol (MeOH) were received from Sigma-Aldrich, while *n*-decyl methacrylate (DMA) was obtained from Polysciences, Inc. (Warrington, PA).

Synthesis of Poly(acrylate) Copolymers. Copolymers of PMMA and PNBA (PMMA:PNBA), PMMA and PIDA (PMMA:PIDA), and PMMA and PDMA (PMMA:PDMA) were included in this study. They were synthesized from solutions containing the following wt % of the monomers: (i) PMMA:PNBA (MMA:NBA = 20:80 and MMA:NBA = 40:60), (ii) PMMA:PIDA (MMA:IDA = 35:65 and MMA:IDA = 45:55, and (iii) PMMA:PDMA (MMA:DMA = 20:80).

The PMMA:PDMA polymer was synthesized following the procedure described by Qin et al.[34] All copolymers were synthesized by thermally initiated free-radical solution polymerization. First, the inhibitors were removed from the monomers by washing with a caustic solution containing 5% (w/v) NaOH and 20% NaCl in a 1:5 (monomer:caustic solution) ratio. The monomers were then washed with water, dried on anhydrous Na_2SO_4, and filtered. AIBN was recrystallized from MeOH before use.

To synthesize PMMA:PNBA and PMMA:PIDA, 25 mL of toluene was added to the monomer mixture (20 g), and the solution was purged with argon for 20 min. The temperature was raised to 84−87 °C, and the polymerization was initiated by adding 50 mg of AIBN. The temperature was maintained within this range for 24 h, while oxygen free atmosphere was maintained by a constant flow of argon. After removing the unreacted monomers under vacuum, the polymer was cooled to room temperature and dissolved in 20 mL THF. Then 100 mL MeOH was added, and the solution was vigorously stirred for 10 min. The polymer was separated from the MeOH, and the process was repeated. Finally, the residual solvent was removed under vacuum.

ISM Preparation. The ISMs were prepared by solution casting of THF solutions, which contained all the membrane components, on zinc selenide (ZnSe) crystals (Crystran Ltd., U.K.). The ZnSe crystals were washed with acetone and cleaned in a plasma cleaner (Harrick) for at least 15 min before solution casting the ISMs on the crystals. The dry weight of the THF solutions was 20 wt %. After deposition, the PA membranes were allowed to dry overnight and the SR membranes for three days before the FTIR-ATR measurements were started. The membrane thicknesses were measured with a micrometer (precision, 1 μm) by placing the membrane-coated ZnSe crystal between two clean microscopic slides. The thicknesses of the bare ZnSe crystal and the two microscopic slides were known and consequently, the ISM thickness could be calculated.

No delamination of the PA and SR membranes from the ZnSe substrate was observed. The PA membranes were very sticky and therefore so well attached to the ZnSe crystals that their full removal after the measurements were difficult. The SR membranes were even more difficult to remove from the ZnSe crystals and were mechanically removed after letting the membranes swell in xylene. This indicates that the PA and SR membranes had good adhesion to the underlying substrate material, and artifacts arising from delamination of the membranes can be excluded.

FTIR-ATR Measurements. The FTIR-ATR measurements and experimental setup have been described in detail elsewhere.[19] The ZnSe crystal covered with the ISM was mounted with an O-ring against an empty Teflon cell (inner volume 0.3 mL), which had been dried at approximately 100 °C for 1 h. An evanescent standing wave is formed within the surface region of the ISM when the IR beam is reflected at the ZnSe−ISM interface. Therefore, the evanescent standing wave can sense the chemical composition (or changes in the composition) of the ISM. The penetration depth was estimated from the Harrick equation[62] to be 0.5−0.6 μm

(47) Kimura, K.; Matsuba, T.; Tsujimura, Y.; Yokoyama, M. *Anal. Chem.* **1992**, *64*, 2508–2511.
(48) Mostert, I. A.; Anker, P.; Jenny, H. B.; Oesch, U.; Morf, W. E.; Ammann, D.; Simon, W. *Mikrochim. Acta* **1985**, *1*, 33–38.
(49) Pick, J.; Pungor, E.; Vasak, M.; Simon, W. *Anal. Chim. Acta* **1973**, *64*, 477–480.
(50) Cha, G. S.; Liu, D.; Meyerhoff, M. E.; Cantor, H. C.; Midgley, A. R.; Goldberg, H. D.; Brown, R. B. *Anal. Chem.* **1991**, *63*, 1666–1672.
(51) Marrazza, G.; Mascini, M. *Electroanalysis* **1992**, *4*, 41–43.
(52) Poplawski, M. E.; Brown, R. B.; Rho, K. L.; Yun, S. Y.; Lee, H. J.; Cha, G. S.; Paeng, K. J. *Anal. Chim. Acta* **1997**, *355*, 249–257.
(53) Yoon, I. J.; Lee, D. K.; Nam, H.; Cha, G. S.; Strong, T. D.; Brown, R. B. *J. Electroanal. Chem.* **1999**, *464*, 135–142.
(54) Turner, D. T. *Polymer* **1987**, *28*, 293–296.
(55) Czanderna, A. W.; Thomas, T. M. *J. Vac. Sci. Technol., A* **1987**, *5*, 2412–2416.
(56) Fyfe, C. A.; Randall, L. H.; Burlinson, N. E. *J. Polym. Sci., Part A: Polym. Chem.* **1993**, *31*, 159–168.
(57) Chu, L. Q.; Mao, H. Q.; Knoll, W. *Polymer* **2006**, *47*, 7406–7413.
(58) Bellucci, F.; Nicodemo, L. *Corrosion* **1993**, *49*, 235–247.
(59) Sammon, C.; Deng, C. S.; Mura, C.; Yarwood, J. *J. Mol. Liq.* **2002**, *101*, 35–54.
(60) Fieldson, G. T.; Barbari, T. A. *Polymer* **1993**, *34*, 1146–1153.
(61) Sammon, C.; Mura, C.; Yarwood, J.; Everall, N.; Swart, R.; Hodge, D. *J. Phys. Chem. B* **1998**, *102*, 3402–3411.
(62) Harrick, N. J. *Internal Reflection Spectroscopy*; Interscience Publishers: New York, 1967.

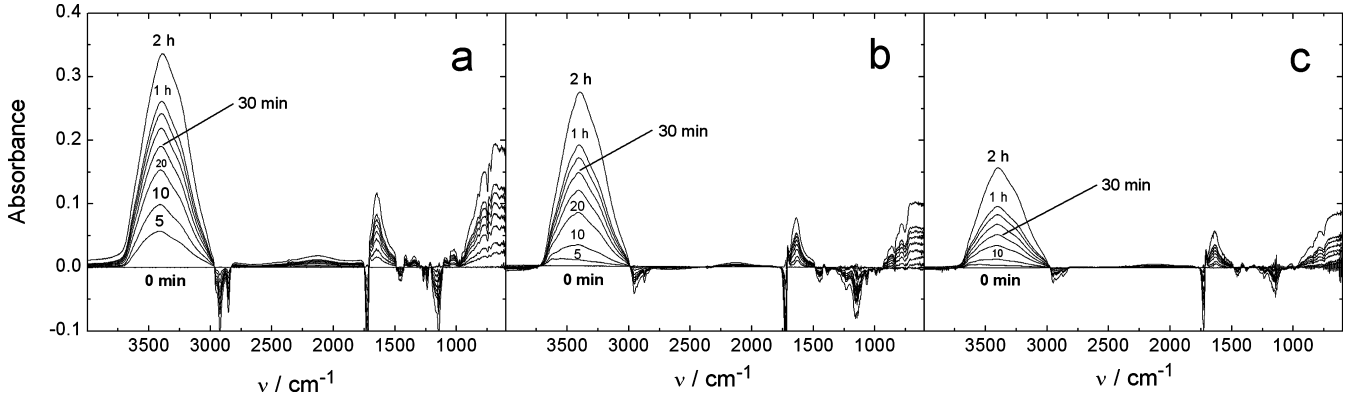

Figure 1. FTIR-ATR spectra of poly(acrylate) membranes consisting of copolymers of (a) PMMA:PDMA (20:80), membrane thickness is 72 μm; (b) PMMA:PNBA (40:60), membrane thickness is 77 μm, and (c) PMMA:PIDA (45:55), membrane thickness is 80 μm. Contact time with deionized water is 2 h.

($n_{1,ZnSe} = 2.43$; $n_{2,PMMA} = 1.489$; $n_{2,RTV3140} = 1.46$) for the PA and SR membranes in the wavenumber region of 3000−3700 cm^{-1}, which corresponds to the region of the OH stretching bands of water.

Before starting the FTIR-ATR measurements, the sample compartment was purged with dry air for 30 min. The background spectrum of the polymer membrane was measured with an empty cell (without water) as well as the first FTIR spectrum in the measurement sequence. Thus, the first spectrum is a straight line with the absorbance value of zero. After measuring the first spectrum, the cell was filled with deionized water within 10 s by using a syringe connected to the outlet (Teflon) tube of the FTIR cell. The FTIR spectra were measured with either 20 or 60 s intervals during the first 2 h of the measurements. In cases where the measurement time was extended to 24 h, the FTIR spectra were measured with 15 min intervals (2−24 h).

The FTIR measurements were conducted with a Bruker IFS 66/S spectrometer equipped with a DTGS detector. The spectra were measured with a resolution of 4 cm^{-1} and either 16 or 32 interferograms were recorded for each spectrum.

Mathematical Modeling of the Diffusion Coefficients. The mathematical modeling of the diffusion coefficients followed the procedure given in detail elsewhere.[19] The diffusion coefficients of water in the PA and SR membranes were calculated with Fick's laws by using the finite difference method and by assuming that the water saturation level was uniform throughout the membrane. In this method, the membrane was divided in N segments with thicknesses of 1 μm. It was assumed that each segment had an individual but uniform concentration. The concentration differences between adjacent segments were used to calculate the concentration profile of water in the membranes at specific times.[48] The wavenumber region of 2470−4800 cm^{-1} was used to deconvolute the OH stretching band of the FTIR spectra (~2960−3750 cm^{-1}) into four different individual water bands: monomeric, dimeric, clustered, and bulk water.[45,61] The OH stretching bands were fitted with 50% Lorentzian and 50% Gaussian peak functions, and the integrated band areas were calculated as the sum of the areas of the four individual water bands. The wavenumber region of ~2960−3750 cm^{-1} was chosen for the determination of the water uptake because it is more easily to distinguish between different types of water in this region, in comparison to the sharp water band at ~1640 cm^{-1}, which overlaps with the (symmetric) water vapor band and partially with the strong C=O stretching bands between 1650−1820 cm^{-1}.

In the FTIR measurements of this study, the measured absorbances of the water at the ZnSe−membrane interface are linearly dependent on the concentration according to the Lambert−Beer law. The finite difference method was applied to simulate time-dependent water concentrations of the Nth segment adjacent to the ZnSe−membrane interface by considering the transmembrane transport and experimentally determined thickness. The diffusion coefficients and saturation levels of water in the membranes were therefore determined by fitting the obtained integrated absorbance versus time curves. It should be noted that the diffusion coefficients might be influenced to a minor extent by swelling of the membrane materials during the FTIR-ATR measurements.

RESULTS AND DISCUSSION

Poly(acrylate) Membranes. The FTIR-ATR spectra of the PMMA:PDMA (20:80), PMMA:PNBA (40:60), and PMMA:PIDA (45:55) membranes, measured during 2 h in contact with water, are shown in Figure 1. The membrane thicknesses were 72, 77, and 80 μm, respectively. When the membranes come into contact with water, water bands with increasing intensities appear in the FTIR spectrum as water diffuses through the membrane and reaches the PA−ZnSe interface. All PA membranes showed a rather fast water uptake, which means that water penetrates all of the studied PA membrane types and reaches the PA−ZnSe interface. The highest water uptake of the PA membranes was observed for the PMMA:PNBA (20:80) (not shown) and PMMA:PDMA (20:80) membranes (Figure 1a). In the FTIR spectrum of the PMMA:PDMA (20:80) membrane, a rather pronounced water band related to OH stretching[63] is already visible in the wavenumber region of ~2960−3750 cm^{-1} after a 5 min contact time with deionized water, which shows that water diffuses very fast through the membrane. The other bands associated with water are located at the wavenumbers of <1000 cm^{-1}, 1643 cm^{-1} (sharp peak due to OH bending vibrations[63]), and 2125 cm^{-1} (broad peak). The downward pointing peaks are associated with PMMA:PDMA and indicate that the molar fraction of PMMA:

(63) Socrates, G. *Infrared and Raman Characteristic Group Frequencies: Tables and Charts*; Wiley: Chichester, U.K., 2001.

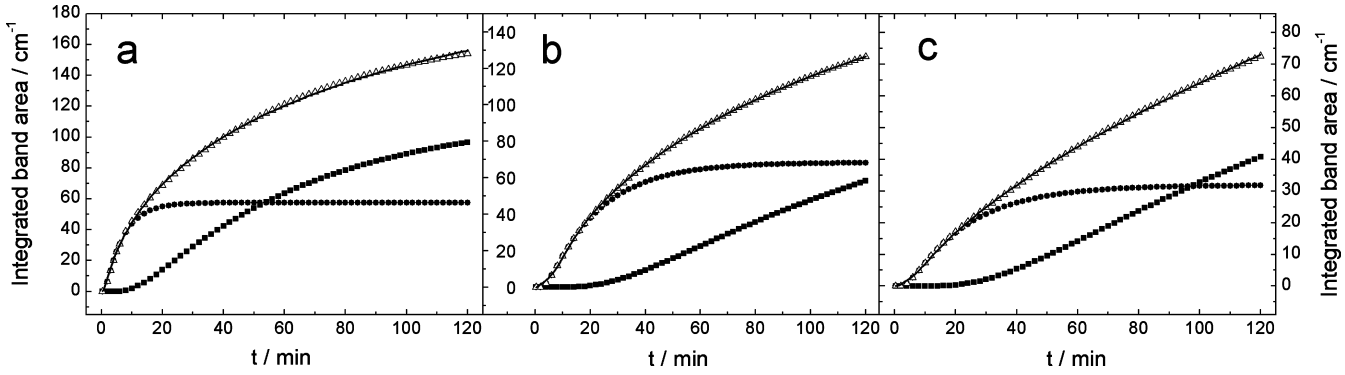

Figure 2. Integrated areas of the OH stretching bands of (a) PMMA:PDMA (20:80), membrane thickness is 72 μm; (b) PMMA:PNBA (40:60), membrane thickness is 77 μm; and (c) PMMA:PIDA (45:55), membrane thickness is 80 μm. Experimentally measured band areas (−) and mathematically simulated band areas for faster (●) and (■) slower diffusion of water through the membranes. Sum of the faster and slower water is indicated with (△).

PDMA at the membrane−ZnSe interface decreases as the water content at this interface increases. The water uptake of the PA and SR membranes in this study is mainly governed by the membranes, which are in direct contact with water. The hydrophobicity of the substrate material may influence the water uptake after a longer time but most likely to a minor extent. However, ZnSe was the substrate material in all FTIR-ATR experiments and should affect the water uptake of all membranes equally.

The water uptake of the PMMA:PNBA (40:60) membrane (Figure 1b) is slightly lower than that of the PMMA:PDMA (20:80) membrane (Figure 1a). This is true especially for the initial water uptake of the PMMA:PNBA (40:60) membrane. The lowest water uptake of all PA membranes was observed for the PMMA:PIDA (35:65) (not shown) and PMMA:PIDA (45:55) membranes (Figure 1c). The water uptake of these membranes was considerably lower than that for the other PA membranes studied. It is not surprising that all of the PAs take up water. It has been reported that low molecular weight PMMA ($M_w = 60600$) takes up about 1.2% water, whereas the water uptake of high molecular weight PMMA was 2.0%.[54] The closer molecular packing of the polymer chains in low molecular weight PMMA was assumed to be the reason for the lower water uptake. About 50% of the water in high molecular weight PMMA was accommodated in microvoids.[64]

The best numerical fittings of the integrated band areas of the OH stretching bands (~2960−3750 cm^{-1}) of the PA membranes (Figure 1) were obtained with a model consisting of two diffusion coefficients, describing faster (D_1) and slower diffusion (D_2) of water in the membranes (Figure 2 and Table 1). Figure 2 reveals that it takes ~20 min for the faster water uptake to reach the equilibrium level in the PMMA:PDMA (20:80) membrane (Figure 2a), whereas it takes ~60 min in the PMMA:PNBA (40:60) and the PMMA:PIDA (45:55) membranes (Figure 2b,c). The faster water is probably related to monomeric and dimeric water and the slower water to clustered and bulk water. The contribution of slower water to the total integrated band area of the PMMA:PDMA (20:80) membrane (Figure 2a) is negligible during the first 10 min of the FTIR measurement, but after that it increases quite rapidly and starts to level off already within 2 h. For the PMMA:PNBA (40:60) and PMMA:PIDA (45:55) membranes it takes much longer (~30 min) before the slower water starts to contribute to the water uptake (total integrated OH stretching band areas) (Figure 2b, c). This indicates that the initial water uptake of these two membranes is lower than that for PMMA:PDMA (20:80).

The diffusion coefficients (D_1 and D_2) obtained by numerical simulations of the integrated absorbances of the OH stretching bands (~2960−3750 cm^{-1}) of the thinner and thicker PA membranes are summarized in Table 1. The diffusion coefficients of PVC:DOS (1:2) membranes have also been included in Table 1.[19] The simulations based on a contact time of 2 h showed that the PMMA:PDMA (20:80) membrane had the highest diffusion coefficients of all the thinner PA membranes studied for the faster (D_1) and slower (D_2) water, 4.7×10^{-8} and 4.9×10^{-9} $cm^2\ s^{-1}$, respectively. However, it should be noted that there are only small differences in the diffusion coefficients of the different PA membranes. In comparison, the diffusion coefficient of water in PMMA was 1.8×10^{-8} $cm^2\ s^{-1}$ ($M_w = 60600$)[54] and 3.2×10^{-9} $cm^2\ s^{-1}$ ($M_w = 130000$).[42] However, Sutandar et al. reported that the diffusion coefficients ranged from 4×10^{-11} to 5×10^{-10} $cm^2\ s^{-1}$ in 5.4 μm thick spin-casted PMMA films.[45] They estimated that the density of sorbed water in PMMA at 100% relative humidity was 0.027 g cm^{-3} (~1.5 M).

One advantage of using the FTIR-ATR technique is that the water content can be measured at the crystal−ISM interface in comparison to that of the gravimetric method, which reflects the water uptake of the entire membrane.[42,54,65,66] According to Fick's laws, the total mass or total concentration change of water has a square root dependence on short times when the mass of the entire membrane is measured. Derivatives of these curves at 0 min are infinite. When there is a water uptake process with two diffusion coefficients, linear regression to the M/M_∞ versus $\sqrt{time}$ dependence only results in one apparent diffusion coefficient of $D_a = (M_{1,\infty}\sqrt{D_1} + M_{2,\infty}\sqrt{D_2})^2/(M_{1,\infty} + M_{2,\infty})^2$, where D_1 and D_2 are the two diffusion coefficients characterizing the slow and fast water uptake, respectively, and $M_{1,\infty}$ and $M_{2,\infty}$ are the saturation values, respectively. Thus, with this method, it is not possible to distinguish between D_1 and D_2. In contrast, when the membrane surface at the crystal−ISM interface is

(64) Turner, D. T. *Polymer* **1982**, *23*, 197–202.
(65) Linossier, I.; Gaillard, F.; Romand, M.; Feller, J. F. *J. Appl. Polym. Sci.* **1997**, *66*, 2465–2473.
(66) Roussis, P. P. *J. Membr. Sci.* **1983**, *15*, 141–155.

Table 1. Diffusion Coefficients and Integrated Absorbances at Infinite Time (A_∞) of Different Types of Poly(acrylate) and Silicone Rubber Membranes[a]

		contact time with water: 2 h				
Poly(acrylate) Membranes	thickness (μm)	D_1 (cm^2 s^{-1})	$A_{1,\infty}$ (cm^{-1})	D_2 (cm^2 s^{-1})	$A_{2,\infty}$ (cm^{-1})	$A_{tot,\infty}$ (cm^{-1})
PMMA:PDMA (20:80)	72	4.7×10^{-8}	57.5	4.9×10^{-9}	114.3	171.8
PMMA:PNBA (40:60)	77	1.7×10^{-8}	68.4	2.3×10^{-9}	128.1	196.5
PMMA:PIDA (45:55)	80	1.7×10^{-8}	31.9	2.1×10^{-9}	103.1	135.0
PVC:DOS (1:2)	107	9.5×10^{-8}	14.1	8.7×10^{-9}	31.6	45.7
PMMA:PDMA (20:80)	316	7.1×10^{-8}	37.3	7.2×10^{-9}	–	–
PMMA:PNBA (40:60)	278	8.9×10^{-8}	7.3	9.5×10^{-9}	–	–
PMMA:PIDA (45:55)	328	5.9×10^{-8}	9.1	7.4×10^{-9}	–	–
PVC:DOS (1:2)	281	3.2×10^{-7}	17.3	4.5×10^{-8}	38.9	56.2
		contact time with water: 24 h				
	thickness (μm)	D_1 (cm^2 s^{-1})	$A_{1,\infty}$ (cm^{-1})	D_2 (cm^2 s^{-1})	$A_{2,\infty}$ (cm^{-1})	$A_{tot,\infty}$ (cm^{-1})
PMMA:PIDA (45:55) +0.45 wt % KTFPB +0.8 wt % ETH5234	324	1.7×10^{-8}	22.0	3.6×10^{-9}	54.7	76.7
PVC:DOS (1:2) +0.45 wt % KTFPB +0.8 wt % ETH5234	317	1.4×10^{-7}	29.1	1.2×10^{-8}	22.4	51.5
		contact time with water: 24 h				
Silicone Rubber Membranes	thickness (μm)	D_1 (cm^2 s^{-1})	$A_{1,\infty}$ (cm^{-1})	D_2 (cm^2 s^{-1})	$A_{2,\infty}$ (cm^{-1})	$A_{tot,\infty}$ (cm^{-1})
RTV 3140	317	2.3×10^{-7}	3.5	9.0×10^{-9}	7.7	11.2
RTV 3140 +0.45 wt % K TFPB +0.8 wt % ETH5234	299	2.0×10^{-7}	5.9	2.0×10^{-8}	6.1	12.0
RTV 3140:DOS (9:1)	287	2.1×10^{-7}	5.2	8.7×10^{-9}	4.9	10.1
RTV 3140 +0.9 wt % KTFPB +1.0 wt % ETH1001	267	2.2×10^{-7}	9.2	1.3×10^{-8}	7.4	16.6

[a] $A_{1,\infty}$ and $A_{2,\infty}$ are the absorbances at infinite time for the faster (D_1) and slower (D_2) water, respectively. $A_{tot,\infty}$ is the sum of these two absorbances.

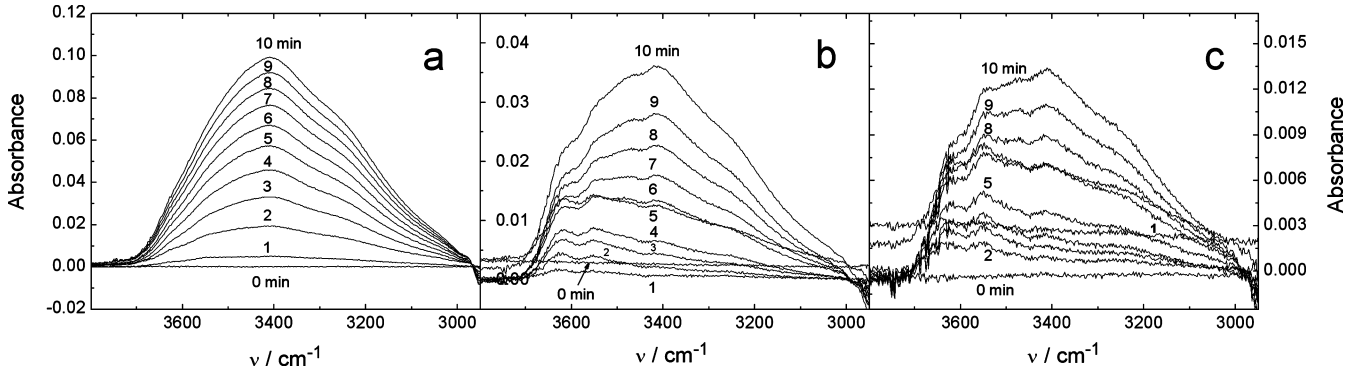

Figure 3. First 10 min of the FTIR-ATR measurements of the poly(acrylate) membranes shown in Figure 1. (a) PMMA:PDMA (20:80), membrane thickness is 72 μm; (b) PMMA:PNBA (40:60), membrane thickness is 77 μm; and (c) PMMA:PIDA (45:55), membrane thickness is 80 μm.

probed with the FTIR-ATR technique, the water reaches the crystal after a certain lag. Derivatives of concentration versus time curves are 0 at 0 min. If the diffusion coefficients of the different water types are different, it is possible to individually assess them by least-squares fittings due to their different lag times.

All diffusion coefficients for the PA membranes are lower than those of the PVC:DOS (1:2) membrane (Table 1). However, the total integrated absorbances at infinitely long times ($A_{tot,\infty}$), which is the sum of the integrated absorbances of the faster and slower water at infinite times ($A_{1,\infty}$ and $A_{2,\infty}$), indicate that the total water uptake of the PA membranes is higher than that for PVC:DOS (1:2). The results in Table 1 show that the PMMA:PNBA (40:60) and PMMA:PDMA (20:80) membranes had the highest water uptake.

The diffusion coefficients for the 2 h measurements of the thicker PA membranes in Table 1 differ slightly from those for the thinner membranes due to the higher uncertainty of the simulated $A_{2,\infty}$ values for the thicker films. For most of the thicker PA membranes, the integrated absorbances of the slower water (A_2) are very small at contact times <60 min. It is therefore impossible to make reliable numerical simulations of $A_{2,\infty}$ for the thicker PA membranes on the basis of FTIR measurements of only 2 h. In this respect, the determination of $A_{2,\infty}$ for the

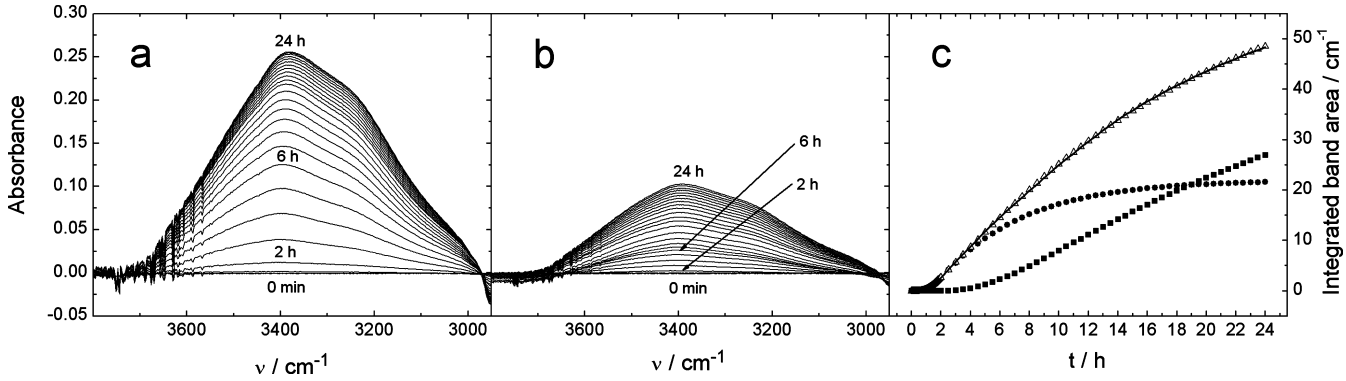

Figure 4. FTIR-ATR spectra of poly(acrylate) membranes consisting of a copolymer of PMMA:PIDA (45:55). (a) Membrane without additives (membrane thickness is 361 μm) and (b) membrane containing 0.8 wt % (10 mmol/kg) ETH 5234 and 0.45 wt % (5 mmol/kg) KTFPB (324 μm). Contact time with deionized water is 2 h. (c) Integrated areas of the OH stretching bands of the spectra shown in panel b. Experimentally measured band areas (−) and mathematically simulated band areas for (●) faster and (■) slower diffusion of water through the membranes. Sum of the faster and slower water is indicated with (△).

thinner PA membranes is much more reliable. For example, in the thinner PMMA:PDMA (20:80) membrane, the slower water already starts to reach an equilibrium level after a contact time of 2 h (Figure 2a).

The FTIR spectra of the thinner PA membranes measured during the first 10 min of the water uptake are shown in Figure 3. The low absorbance values indicate that the PMMA:PIDA (45:55) membrane has the lowest water uptake during the first 10 min (Figure 3c). There are also some differences in the water uptake of the different PA membranes. For the PMMA:PNBA (40:60) and PMMA:PIDA (45:55) membranes, the bands originating from monomeric (~3625 cm^{-1}) and dimeric (~3560 cm^{-1}) water dominate the spectra after 2 min (Figure 3b,c).[45] Only very weak and broad bands of the clustered (~3420 cm^{-1}) and bulk (~3250 cm^{-1}) water are visible in the FTIR spectra. After 10 min, the monomeric and dimeric bands have shifted to slightly lower wavenumbers (lower frequencies) of ~3620 and ~3540 cm^{-1}, respectively, which indicates a higher degree of network formation of water in these membranes.[19,45,61] This is supported by the fact that the relative amount of dimeric water in the PMMA:PNBA (40:60) and PMMA:PIDA (45:55) membranes also increases with time in comparison to that of the monomeric water band, besides the significant increase of the clustered and bulk water bands. The peak position of the clustered water band shifts to only slightly lower wavenumbers (~3415 cm^{-1}), whereas the bulk water band is practically unaffected by the measurement time. The band at ~3475 cm^{-1} has been assigned to the weak overtone of the C=O stretching band of the PA matrix[45,63] and contributes to some extent to the total integrated absorbance (A_{tot}). However, the C=O stretching vibrations of the dry PA membranes are eliminated from the FTIR spectra by measuring the background before starting the FTIR-ATR measurement (Experimental Section). In ref 45, FTIR analysis of 100 nm thick PMMA films showed that the weak C=O overtone band at 3452 cm^{-1} remained constant during the water uptake study (1 h). Its relative peak area was only 0.1% in comparison to the strong bulk water band at about 3300 cm^{-1}. It is therefore assumed that the relative contribution of the C=O overtone band at ~3475 cm^{-1} to the total integrated OH stretching band area in this study (~2960−3750 cm^{-1}) is not significant.

In the PMMA:PDMA (20:80) membrane (Figure 3a), the relative contribution of the monomeric and dimeric water is much lower during the first 10 min compared to that of the PMMA:PNBA (40:60) and PMMA:PIDA (45:55) membranes. Clustered water (~3420 cm^{-1}) is already the dominating species in the PMMA:PIDA membrane after a contact time of 2 min. The dimeric water (~3540 cm^{-1}) dominates over monomeric water (~3620 cm^{-1}), and the bulk water band (~3245 cm^{-1}) is much more pronounced than in the PMMA:PNBA (40:60) and PMMA:PIDA (45:55) membranes after the same contact time. It is therefore reasonable to assume that there are differences in the initial water uptake of the PMMA:PDMA (20:80) membrane and the two other PA membranes shown in Figure 3.

The PMMA:PIDA (45:55) membrane was studied more extensively because it has the lowest water uptake of all the PA membranes. The water uptake of a thicker PMMA:PIDA (45:55) membrane (thickness, 361 μm) was therefore measured for 24 h (Figure 4a). It was observed that the water uptake almost completely levels off within 24 h. The water uptake of the PMMA:PIDA (45:55) membrane (thickness, 324 μm) was significantly decreased by the addition of 0.45 wt % KTFPB and 0.8 wt % ETH 5234 (calcium ionophore IV) to the membrane matrix (Figure 4b). This was also previously observed for the PVC:DOS (1:2) membranes.[19] Figure 4c shows that the faster water (D_1) reached the equilibrium level in the membrane within ~12 h. However, the slower water (D_2) did not reach the equilibrium level even after 24 h. Table 1 reveals that the diffusion coefficient of the faster water (D_1) is identical (1.7×10^{-8} cm^2 s^{-1}) for the thinner and thicker PMMA:PIDA (45:55) membranes, and only a slight difference is observed in the diffusion coefficients of the slower water, 2.1×10^{-9} and 3.6×10^{-9} cm^2 s^{-1}, respectively. The numerical simulations based on the FTIR-ATR data obtained during 24 h should be the most reliable. For comparison, the diffusion coefficients and integrated absorbance values of a PVC:DOS (1:2) membrane containing 0.45 wt % KTFPB and 0.8 wt % ETH 5234, based on 24 h measurements, have been included in Table 1.[19] The table shows that D_1 of the PMMA:PIDA (45:55) membrane, containing KTFPB and ETH 5234, is approximately 1 order of magnitude lower than that of the PVC:DOS membrane, and that D_2 is considerably lower for the

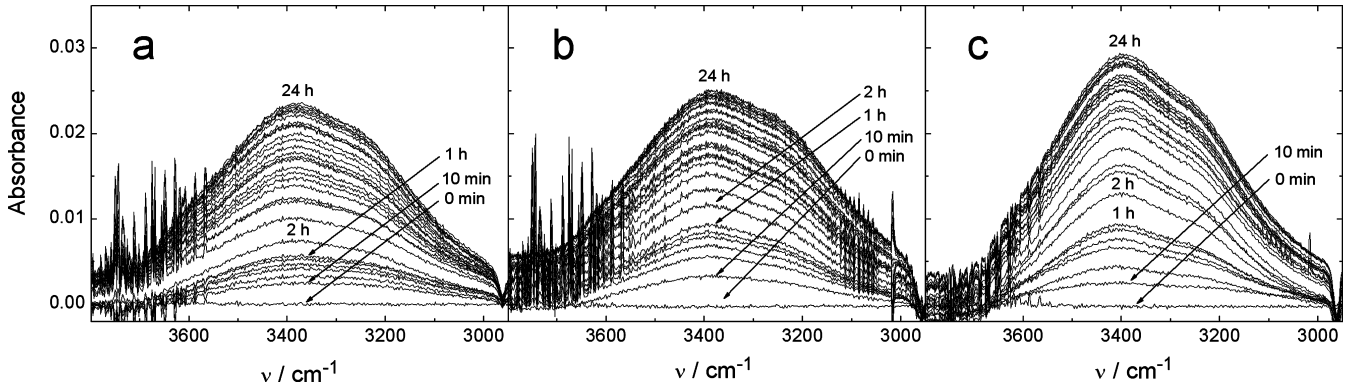

Figure 5. FTIR-ATR spectra of a silicone rubber (RTV 3140) membrane containing (a) no additives, membrane thickness is 317 μm; (b) 10 wt % DOS (RTV 3140:DOS, 9:1), membrane thickness is 287 μm; and (c) 0.45 wt % (5 mmol/kg) KTFPB and 0.80 wt % (10 mmol/kg) ETH 5234, membrane thickness is 299 μm. Contact time with deionized water is 24 h.

PMMA:PIDA membrane. This confirms that the diffusion of water is much slower in the PMMA:PIDA membrane than that in the PVC:DOS membrane. However, the $A_{tot,\infty}$ value indicates that at equilibrium the total water uptake of the PMMA:PIDA membrane containing KTFPB and ETH 5234 is higher than that for the PVC:DOS membrane of the same thickness containing the same additives. However, it should be noted that at short contact times, less than 2 h, the water uptake of the PMMA:PIDA membrane (Figure 4b,c) is much lower than that for the PVC:DOS membrane.[19]

Silicone Rubber Membranes. The FTIR spectra of a 317 μm thick SR membrane (containing no additives) are shown in Figure 5a. A water band can already be observed after 10 min, indicating that water diffuses through the membrane. However, the value of the absorbance maximum of the SR membrane after 24 h is approximately only one tenth of the absorbance maximum of the PMMA:PIDA (45:55) membrane with the same thickness (Figure 4a). The absorbance maximum of a 103 μm thick SR membrane (containing no additives) was approximately 0.045 absorbance units after 24 h. It shows that the water uptake of the SR membranes is much lower than that of the PA and plasticized PVC membranes.[19] This conclusion is also supported by the low $A_{tot,\infty}$ value (11.2 cm^{-1}) of the 317 μm thick SR membrane (Table 1). No weight increase was observed for the SR membrane containing no additives after soaking it in deionized water for 96 h, whereas the weight of the PVC:DOS (1:2) and the PMMA:PIDA (45:55) membranes increased slightly (0.25−0.3 wt %). However, simply weighing the membranes is not precise enough, and a more accurate method should be used to determine the water content of the membranes. Although the significant water uptake of SR membranes may seem surprising, there are earlier reports on water uptake of different types of SRs and the influence of additives on the water uptake.[67,68] It was shown that the diffusion coefficient of water in a membrane without additives was 1.1×10^{-7} cm^2 s^{-1} but could vary between 4.7×10^{-10} and 2.7×10^{-8} cm^2 s^{-1}, depending on the amount of additives (0.6−16.0 wt %) in the SR membranes. The additives also increased the water uptake from 0.09 wt % (SR without additives) to 1.52 wt %. Even different silicone rubbers used for high voltage insulations showed a relatively high water uptake by gravimetric methods.[69]

The FTIR measurements also indicate that the addition of 10 wt % DOS (Figure 5b) or 0.45 wt % KTFPB and 0.8 wt % ETH 5234 (Figure 5c) does not influence the water uptake ($A_{tot,\infty}$) of the SR membranes to any greater extent (Table 1). This is partially in contradiction with the observation that DOS increases the water uptake and that the addition of KTFPB and ETH 5234 slows down the water uptake of plasticized PVC[19] and PMMA:PIDA (45:55) membranes. However, the small differences in the measured absorbances in Figure 5a−c and the slight variations in the membrane thicknesses (287−317 μm) make it difficult to draw any definite conclusions about the differences in the water uptake of the SR membranes. Only minor differences were observed in the $A_{tot,\infty}$ values of the three different SR membranes (10.1−12.0 cm^{-1}).

Interestingly, the diffusion coefficients of the faster ($D_1 \approx 10^{-7}$ cm^2 s^{-1}) and slower ($D_2 \approx 10^{-8}$ cm^2 s^{-1}) water are almost similar for all of the SR membranes, the PVC:DOS (1:2) membrane (contact time with water, 2 h), and the PVC:DOS membrane containing 0.45 wt % KTFPB and 0.8 wt % ETH 5234 (contact time, 24 h) (Table 1). This means that the water uptake proceeds with the same rate in these membranes, but the $A_{tot,\infty}$ values reveal that the water uptake of the SR membranes is much lower than that of plasticized PVC membranes. It should be pointed out that the numerical fittings of the FTIR data for the SR membranes shown in Figure 6a−c are quite good but not completely perfect, even though the model with two diffusion coefficients gave the best fit. However, the integrated absorbances of the OH stretching bands indicate that the water uptake of the PMMA:PIDA (45:55) membrane containing KTFPB and ETH 5234 (Figure 4c) is lower than that of the SR membranes during the first 2 h (Figure 6). This is supported by the fact that the diffusion coefficients of water is approximately 1 order of magnitude lower for the PMMA:PIDA (45:55) membrane containing KTFPB and ETH 5234 than those of the SR membrane containing the same additives.

Unlike the SR membrane containing 0.45 wt % KTFPB and 0.8 wt % ETH 5234, the addition of 0.9 wt % KTFPB and 1.0 wt %

(67) Watson, J. M.; Baron, M. G. *J. Membr. Sci.* **1996**, *110*, 47–57.
(68) Riggs, P. D.; Parker, S.; Braden, M.; Kalachandra, S. *Biomaterials* **1997**, *18*, 721–726.
(69) Dowling, K.; Hillborg, H. 1999 Annual Report Conference on Electrical Insulation and Dielectric Phenomena (Cat. No.99CH36319), Institute of Electrical and Electronics Engineers (IEEE): Austin, TX, 1999; Vol. 341, pp 342−345.

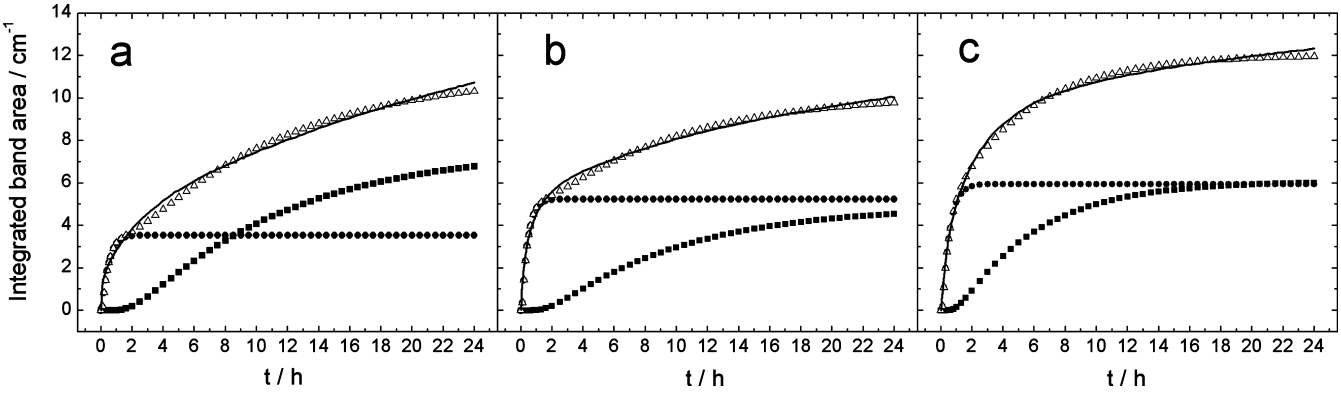

Figure 6. Integrated areas of the OH stretching bands of the silicone rubber (RTV 3140) membrane containing (a) no additives, membrane thickness is 317 μm; (b) 10 wt % DOS (RTV 3140:DOS, 9:1), membrane thickness is 287 μm, and (c) 0.45 wt % (5 mmol/kg) KTFPB and 0.80 wt % (10 mmol/kg) ETH 5234, membrane thickness is 299 μm. Experimentally measured band areas (−) and mathematically simulated band areas for (●) faster and (■) slower diffusion of water through the membranes. Sum of the faster and slower water is indicated with (△).

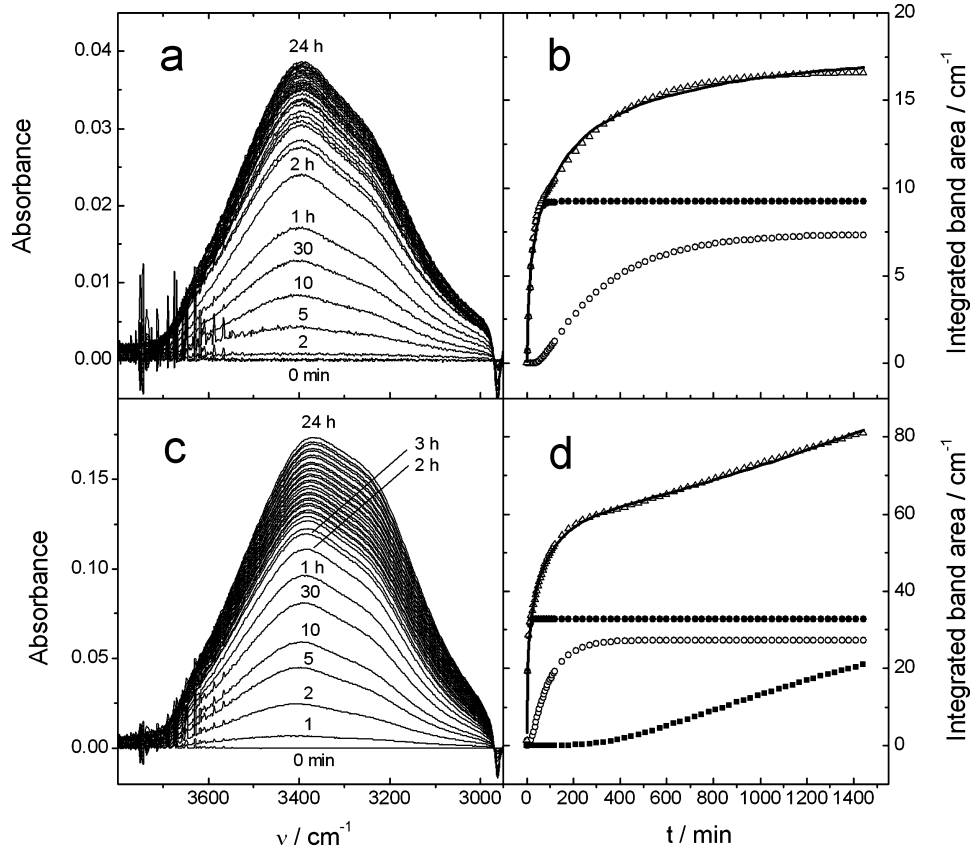

Figure 7. FTIR-ATR spectra of SR membranes containing 0.9 wt % (10 mmol/kg) KTFPB and 1.0 wt % (14.6 mmol/kg) ETH 1001; membrane thicknesses: (a) 267 μm and (c) 109 μm. The membranes were in contact with water for 24 h. The integrated areas of the OH stretching bands in figures (a) and (c) are shown in (b) and (d), respectively. Experimentally measured band areas (−) and mathematically simulated band areas for (•) fast, (○) slow, and (■) the slowest diffusion of water through the membranes. The sum of the band areas is indicated with (△).

ETH 1001 to the SR membrane increased the water uptake (Figure 7). This membrane formulation has previously been used in Ca^{2+}-selective SR membranes.[70] The water uptake of a 267 μm thick SR membrane containing KTFPB and ETH1001 is low, and most of the water uptake takes place during the first 5 h of the measurement and then levels off almost completely within 24 h (Figure 7a,b). The water uptake is slightly higher than that of the SR membrane containing 0.45 wt % KTFPB and 0.8 wt % ETH 5234. Numerical simulations showed that the diffusion of water in the 267 μm thick SR membrane could be best described with two diffusion coefficients, $D_1 = 2.2 \times 10^{-7}$ cm^2 s^{-1} and $D_2 = 1.3 \times 10^{-8}$ cm^2 s^{-1}, respectively (Table 1). The integrated absorbance of the OH stretching bands (~2960−3750 cm^{-1}) at an infinite time ($A_{tot,\infty}$) is 16.6 cm^{-1}, which is slightly higher than that of SR membranes containing either no additives or 0.45 wt % KTFPB and 0.8 wt % ETH 5234.

(70) Malinowska, E.; Oklejas, V.; Hower, R. W.; Brown, R. B.; Meyerhoff, M. E. *Sens. Actuators, B* **1996**, *33*, 161–167.

However, the water uptake of a 109 μm thick SR membrane is rather high, $A_{tot,\infty} = 111.6\ cm^{-1}$ (Figure 7c,d). The water uptake is very fast during the first 10 min of the FTIR measurement, which is also the case with the thicker membrane, but slows after ~3 h. However, an equilibrium state is not reached even within 24 h. In contrast to the thicker SR membrane, the diffusion of water in the thinner membrane was best described with a model consisting of three diffusion coefficients, $D_1 = 1.4 \times 10^{-7}$ cm^2 s^{-1}, $D_2 = 7.8 \times 10^{-9}$ cm^2 s^{-1}, and $D_3 = 3.4 \times 10^{-10}$ cm^2 s^{-1}, respectively. The first two diffusion coefficients (D_1 and D_2) are approximately of the same order of magnitude as the diffusion coefficients of the thicker SR membrane. However, the third coefficient (D_3) is considerably lower than the second diffusion coefficient (D_2), which shows that a third very slow process is involved in the water uptake of the thinner SR membranes. The exact physicochemical meaning of these diffusion coefficients is still unclear. For the thinner SR membranes, it can be speculated that D_1 is related to the diffusion processes of monomeric and dimeric water and D_2 and D_3 to clustered and bulk water, respectively. However, for the thicker membranes, D_2 probably reflects diffusion of clustered and bulk water. Because evidence for a water-rich surface region spanning from 20 to 40 μm was already reported for PVC-based ISMs,[71] it might be that such a region exists also in SR membranes. This could explain the large difference in the water uptake of the thicker and thinner SR membranes.

The increased water uptake of SR due to the presence of KTFPB and ETH 1001 in the membrane matrix is in contrast to results recently reported for plasticized PVC membranes[19] and the PMMA:PIDA (45:55) membrane in this study. In both cases, KTFPB and ETH 5234 decreased the water uptake of these membranes. It is possible that the additives (ETH 1001, ETH 5234, and KTFPB) are more hydrophobic than plasticized PVC and PMMA:PIDA (45:55) but less hydrophobic than SR. This would explain the differences in the influence of the additives on the water uptake of the different membrane matrixes.

On the basis of the results of the FTIR-ATR measurements, it can be concluded that water diffuses to a certain extent through all SR membranes studied. However, on longer time scales the water uptake of most of the SR membranes is much lower compared to that of the plasticized PVC and PA membranes. This will possibly be favorable for obtaining stable and reproducible SC-ISEs with a low detection limit.

(71) Chan, A. D. C.; Li, X. Z.; Harrison, D. J. *Anal. Chem.* **1992**, *64*, 2512–2517.

CONCLUSIONS

FTIR-ATR spectroscopy has been applied for the first time to study the water uptake of ISMs based on different types of PA and SR membranes. All studied membranes take up water resulting in the presence of water at the polymer−ZnSe interface. Numerical simulations using the finite difference method showed that the water uptake of the PA and most of the SR membranes is best described by a model including two diffusion coefficients.

The diffusion coefficients of the faster and slower water in the PA membranes were approximately 1 order of magnitude lower than those of PVC:DOS (1:2) membranes, whereas the total water uptake of the PA membranes at infinitely long times was higher roughly with a factor of 1.5 than that of the PVC:DOS (1:2) membranes.

The diffusion coefficients of the SR membranes were almost the same as for plasticized PVC membranes. However, the SR membranes had the lowest water uptake of all membranes studied, which can be advantageous in the development of SR-based SC-ISEs with a low detection limit. It was observed that ETH 1001 and KTFPB increased the water uptake of SR membranes.

The high sensitivity of the FTIR-ATR technique for different types of water combined with the finite difference method, which can address complex mass transport problems, show promise for assessing water uptake in a wider range of applications than ISMs.

ACKNOWLEDGMENT

F.S. and T.L. gratefully acknowledge the Academy of Finland and the Hungarian Academy of Sciences for financial support. This work was partially financed by the Hungarian Scientific Fund (OTKA NF 69262) and is also a part of the activities of the Åbo Akademi Process Chemistry Centre within the Finnish Centre of Excellence Program (Academy of Finland, 2000-2011). The authors thank Dr. Beatriz Meana-Esteban for helpful discussions about the FTIR-ATR technique.

NOTE ADDED AFTER ASAP PUBLICATION

This manuscript originally posted ASAP June 15, 2009. The layout of Table 1 was modified, and the corrected version posted ASAP on June 19, 2009.

Received for review April 6, 2009. Accepted May 29, 2009.

AC900727W